PDE Transform --- A unified paradigm for data analysis and multiscale modeling

Guowei Wei

Department of Mathematics

Center for Mathematical Molecular Biosciences

Michigan State University

http://www.math.msu.edu/~wei

2014 International Conference on Modeling of Complex Biological Systems

Nankai University, May 26-29, 2014

Grant support:

NIH R01GM, NSF DMS (Focus Research Group), CCF, IIS Michigan State University

Diffusion equation for image processing

(Withkin 1983)

$$u_t(r,t) = d\nabla^2 u(r,t)$$

$$u(r,0) = I(r)$$

Constant

Scale-space filter
Gaussian filter

Original

Original+Noise

Processed with the diffusion equation

Perona-Malik equation (1990)

$$\frac{\partial u}{\partial t} = \nabla \bullet \left[d\left(|\nabla u|\right) \nabla u \right],$$

$$u(r, t=0) = I(r)$$

Gradient dependent

$$d\left(|\nabla u|\right) = \exp\left(-\frac{|\nabla u|^2}{2\sigma^2} \right), \qquad or$$

$$d\left(|\nabla u|\right) = \frac{1}{1+|\nabla u|^2}$$

Mean Curvature Flow

Osher & Sethian (1988); Chan,…

Original

Geometric evolution equation

Osher and Sethian (1988)
Mumford-Shah (1989)
Ruidin, Osher & Fatemi (1992)
Catte, Lions, Morel & Coll (1992)
Nitzberg & Shiota (1992)
You, Xu, Tannenbaum & Kaveh (1996)
Acton (1996)
Sapiro (1996)
Torkamani-Azar & Tait (1996)
Kichenassamy (1997)
Blomgren & Chan (1998), Chan & Vese (2001)
Bajaj & Xu (2005)
******

Incomplete list

The first high-order stochastic geometric PDEs introduced for image analysis

Wei (IEEE SPL 1999); Greer & Bertozzi (2004); Gilboa, Sochen & Zeevi (2004); Xu and Zhou (2007); ....

$$\frac{\partial u}{\partial t} = \sum_{j=0} \nabla \bullet \left[d_j \left(|\nabla u| \right) \nabla \nabla^{2j} u \right] + V \left(|\nabla u| \right),$$

$$u(r, t = 0) = I(r)$$

$$d_0 \left(|\nabla u| \right) = \exp\left(- \frac{|\nabla u|^2}{2\sigma^2} \right),$$

$$\sigma^2 = \overline{\left| \nabla u - \overline{\nabla u} \right|^2}$$

Gradient dependent

Nonlinear term

Stochastic coef.

Use of Cahn-Hilliard type of potential

$$\frac{\partial u}{\partial t} = \nabla \bullet \left[d_1(|\nabla u|) \nabla \nabla^2 u \right] + c(|\nabla u|)(u^2 - u_0^2)u$$

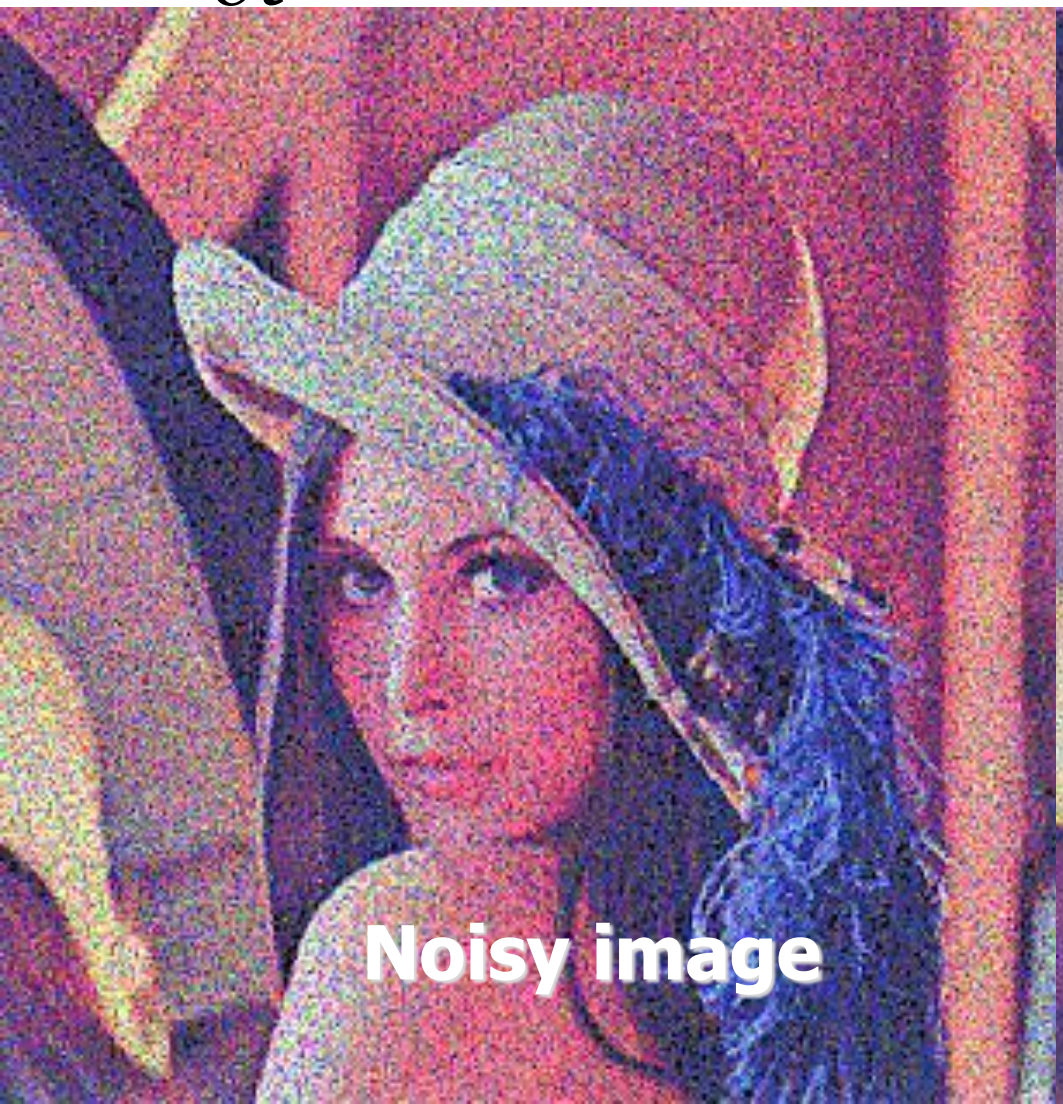

Edge detection using coupled PDEs

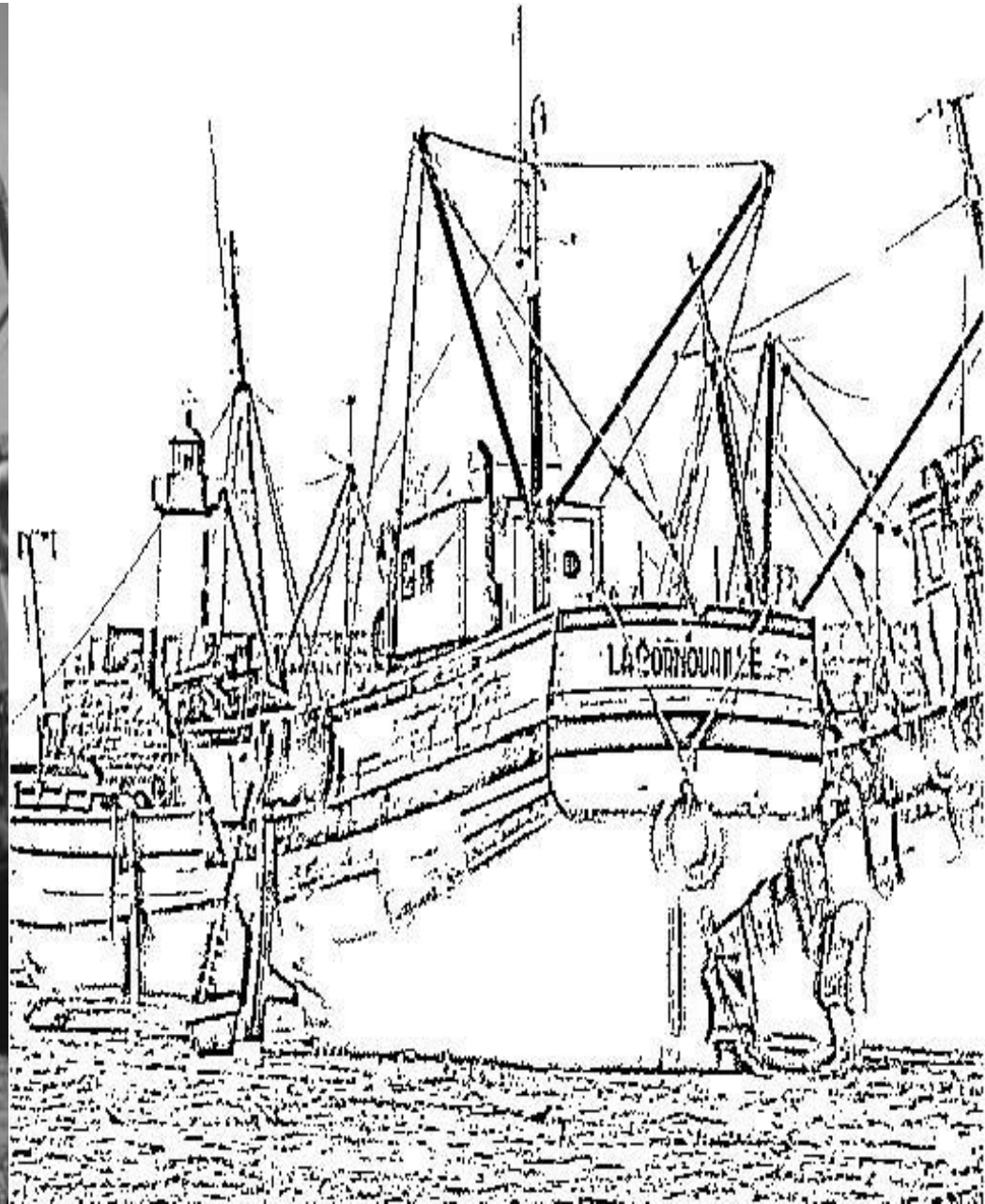

PDE transform for the processing of Cryo-EM data

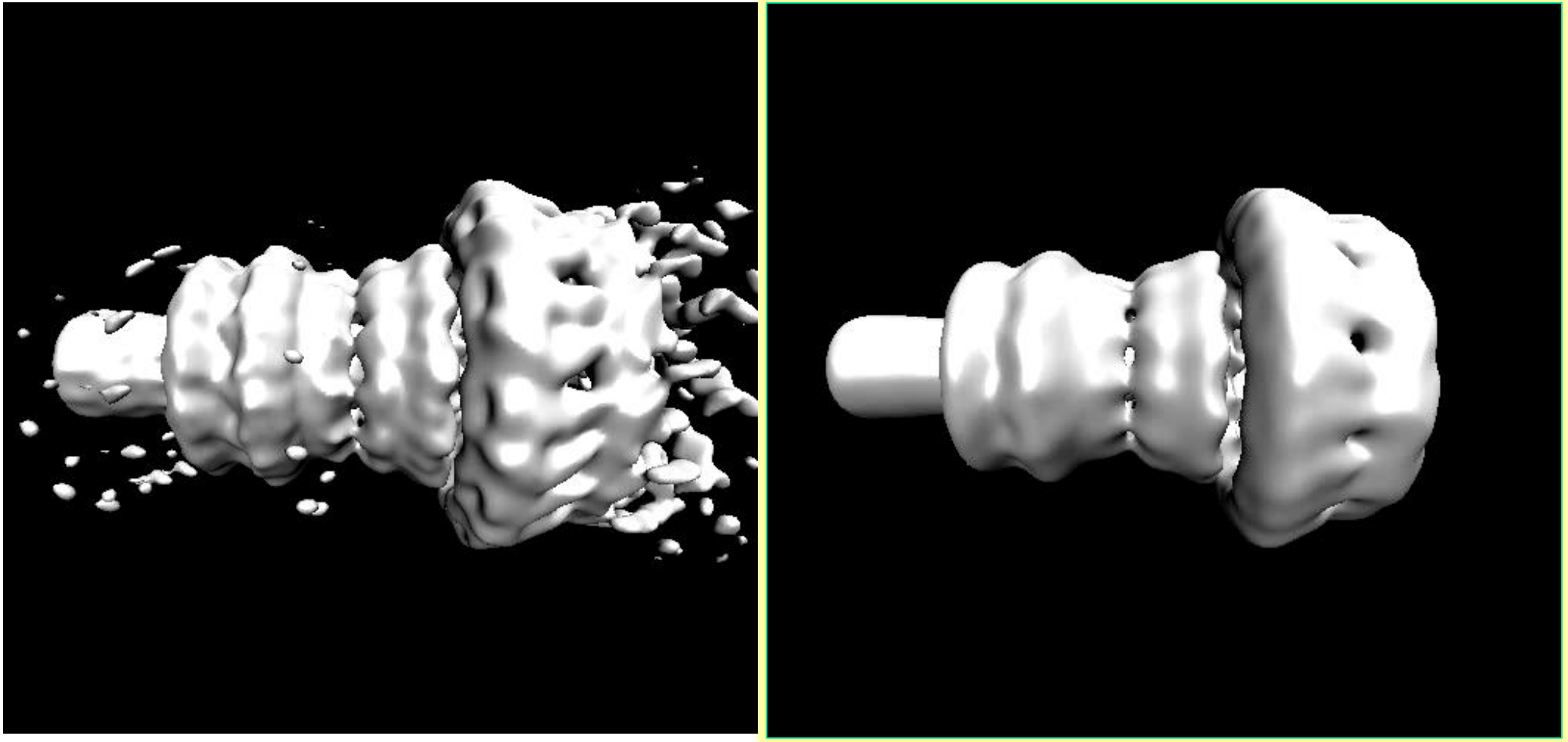

Bacterium Type III secretion system

Feng, Xia, Tong & Wei, IJNMBE, 2012

The first PDE based molecular surface modeling

$$\frac{\partial S}{\partial t} = \sum_{n=0} \nabla \bullet \left[d_n \left(|\nabla S| \right) \nabla \nabla^{2n} S \right] + v\left(|\nabla S| \right)$$

(Wei, IEEE Signal Proc. Lett., 1999)

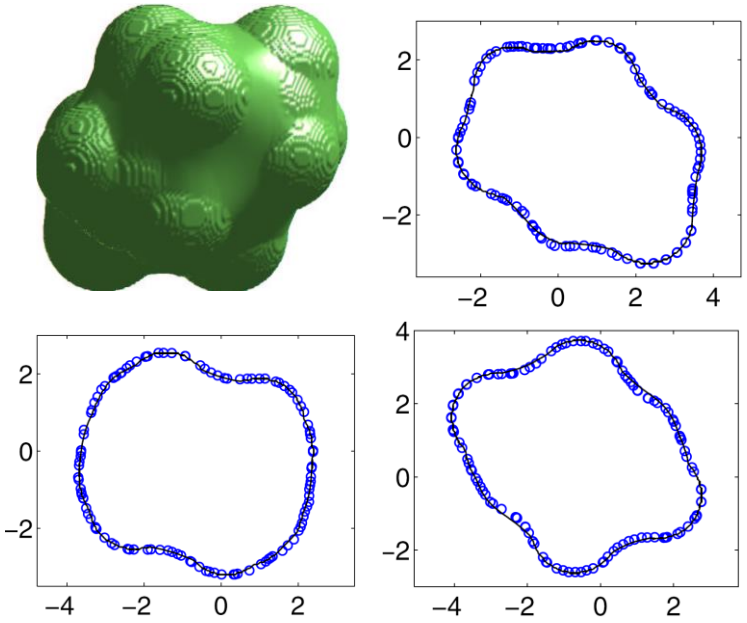

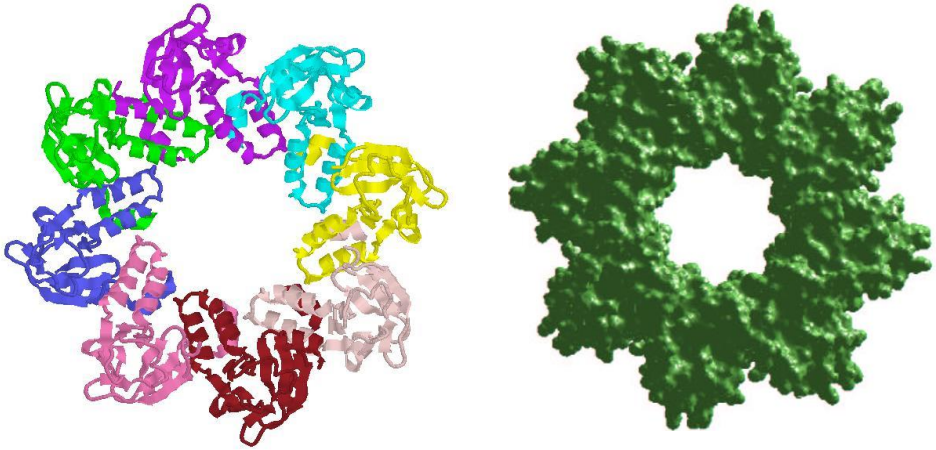

The cell division protein, PDB ID: 1N0E, 9245 atoms in 1328 residues

Major feature: Starting from atomic information, instead of a given surface

(Wei, Sun, Zhou and Feig, 2005)

The first PDE based nonlinear **high-pass filter**

$$\frac{\partial u}{\partial t} = \nabla \bullet \left[d_u \left(|\nabla u| \right) \nabla u \right] + c_u (v - u),$$

$$\frac{\partial v}{\partial t} = \nabla \bullet \left[d_v \left(|\nabla v| \right) \nabla v \right] + c_v (u - v)$$

Relative fidelity

$$u(r, t = 0) = v(r, t = 0) = I(r)$$

$$Edge(E):$$

$$E(r, t) = u(r, t) - v(r, t)$$

Wei & Jia (EPL 2002); Sun,Wu,Wang & Wei (2006)

Original

Coupled PDEs

Wei & Jia (EPL 2002)

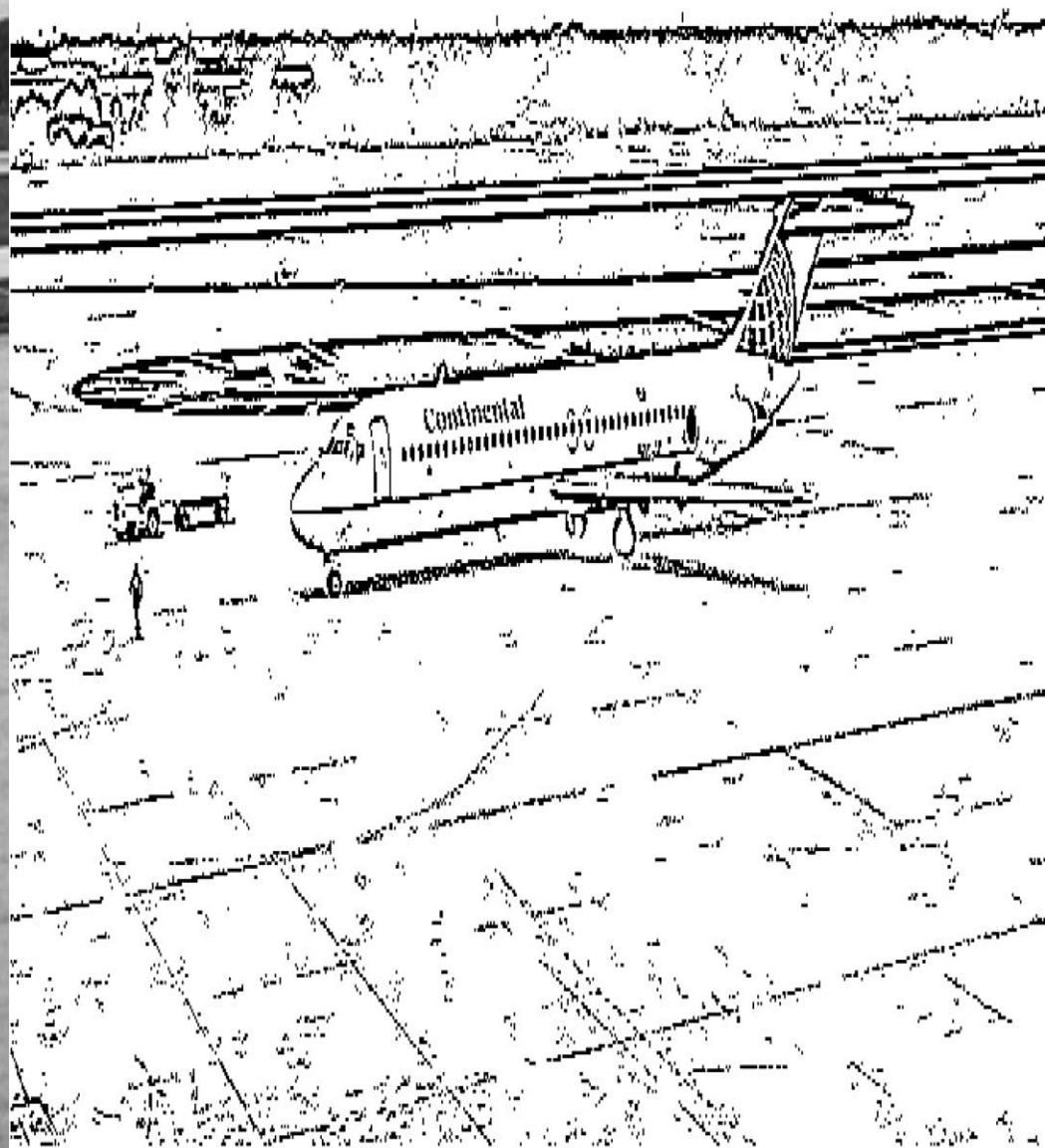

PDE transform

$$\frac{\partial u}{\partial t} = \sum_{i=0}^{n-1} \nabla \bullet \left[d_i \left(|\nabla u| \right) \nabla \nabla^{2i} u \right] + c_u (v - u),$$

$$\frac{\partial v}{\partial t} = \sum_{j=0}^{m-1} \nabla \bullet \left[d_j \left(|\nabla v| \right) \nabla \nabla^{2j} u \right] + c_v (u - v)$$

$$u(r, t = 0) = v(r, t = 0) = I(r)$$

Wang, Wei, Yang, IJNMBE 2011;
Wang, Wei, Yang, JSC, 2012

Intrinsic mode functions (IMFs)

$$w_{nm}^k = u_n - v_m = H_{nm} X^k, \qquad \forall k = 1,2,\ldots$$

$$X_{nm}^1 = I(r)$$

$$X_{nm}^k = X_{nm}^1 - \sum_{l=1}^{k-1} w_{nm}^l, \qquad \forall k = 2,3,\ldots$$

$$I = X_{nm}^k + \sum_{l=1}^{k-1} w_{nm}^l$$

Perfect reconstruction

Frequency response of the PDE transform

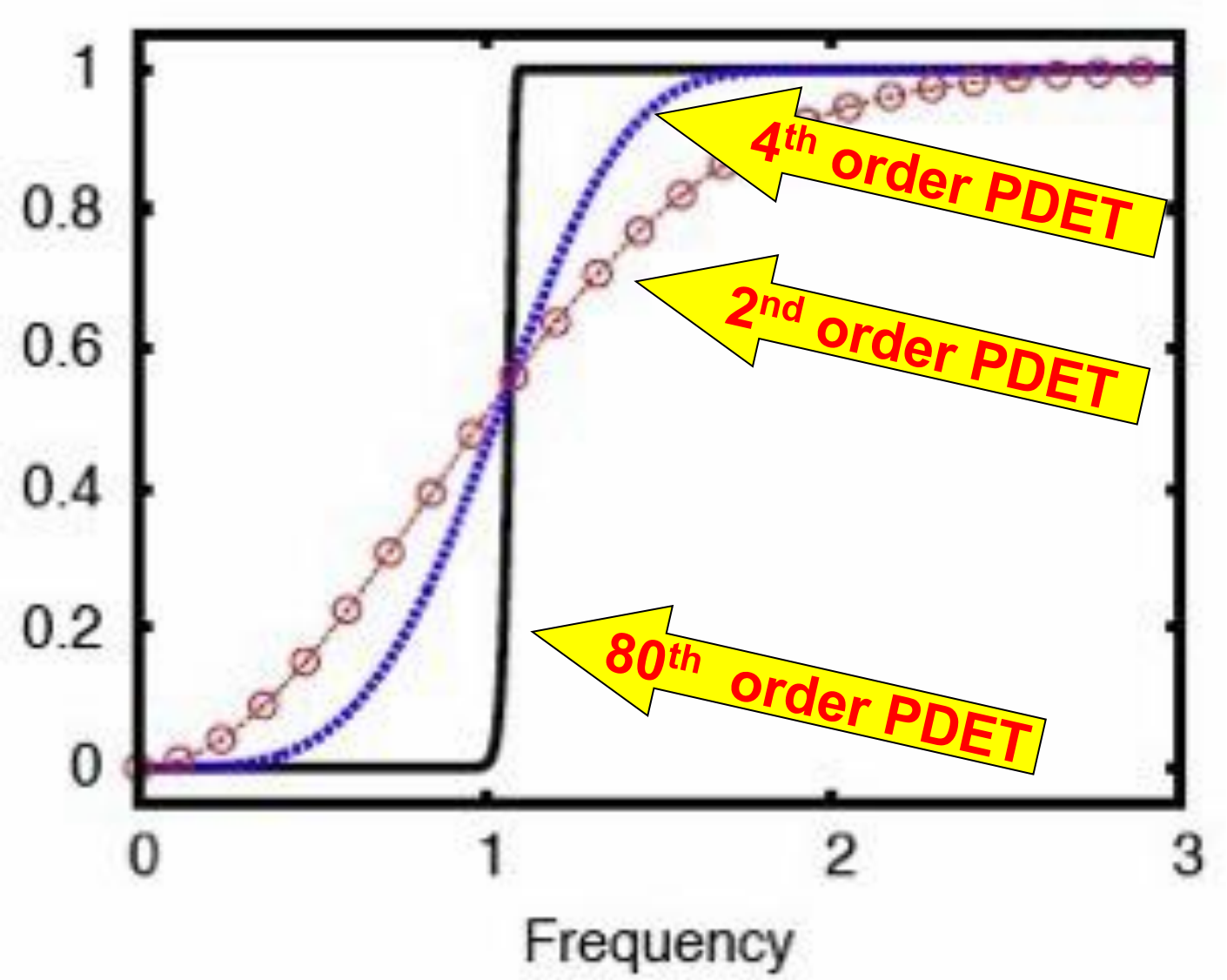

PDE order controls time-frequency localization

(Wang, Wei, Yang, JSC, 2012)

Central Pacific sea surface temperature

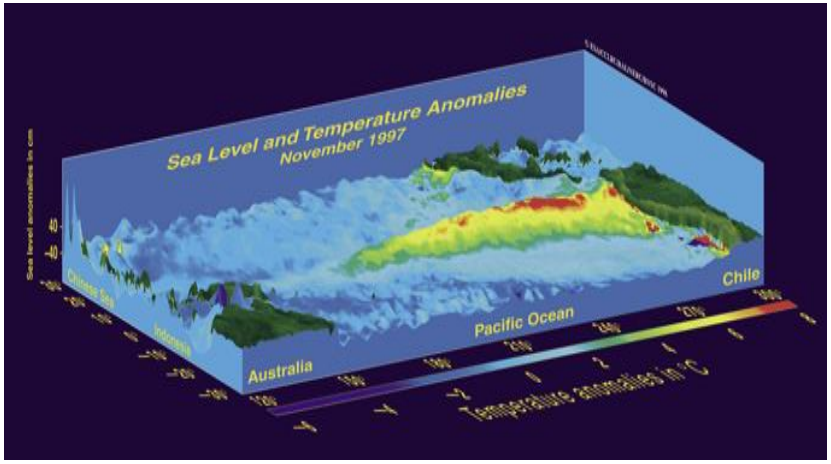

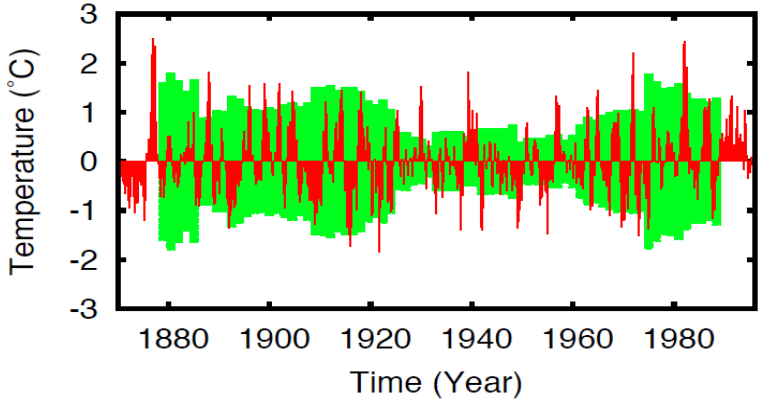

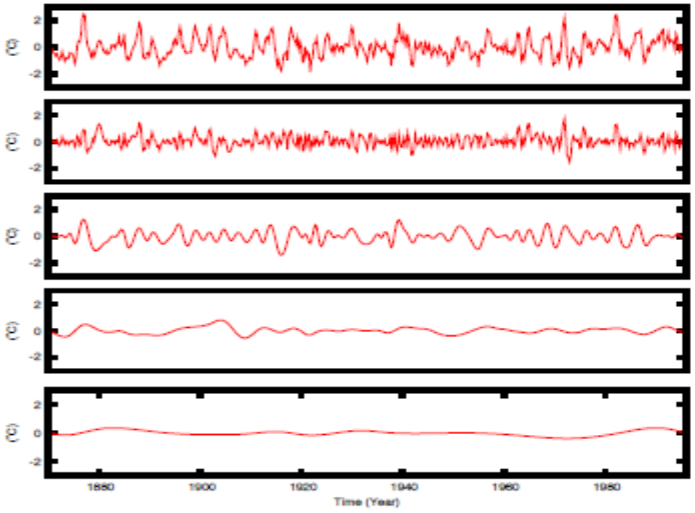

(a) The original SST signal (top panel) and the first four significant intrinsic mode functions generated by the EMD method.

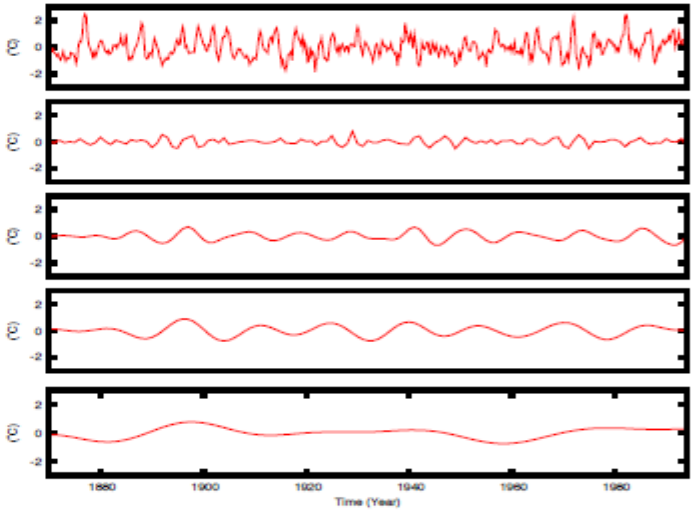

(b) The four modes generated by the PDE transform for the same SST signal on the top panel are similar to those from the EMD decomposition.

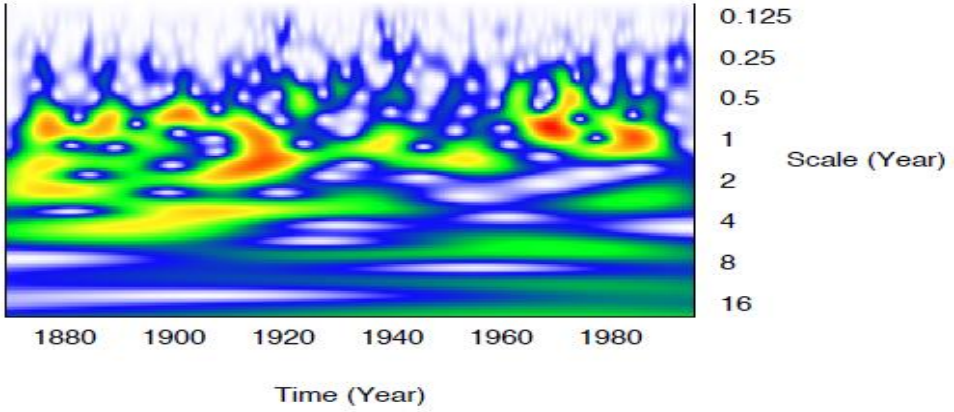

(a) Continuous wavelet analysis of the SST Nino3 data.

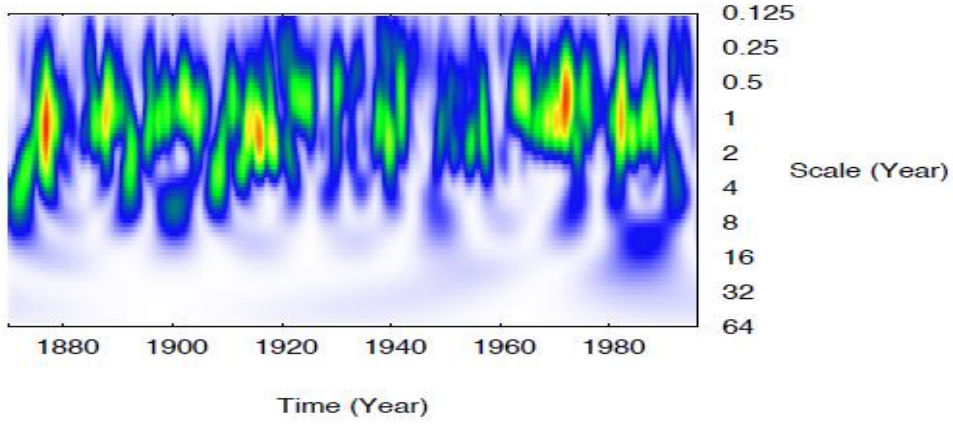

(b) PDE transform using 2nd order PDE.

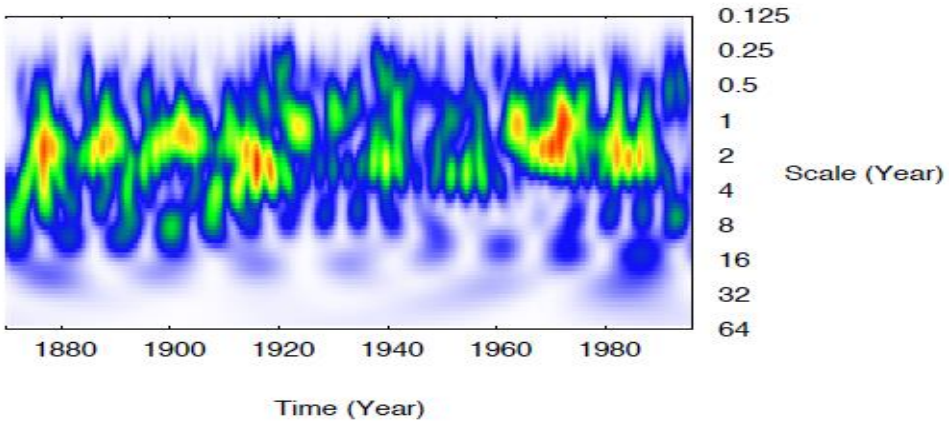

(c) PDE transform using 4th order PDE.

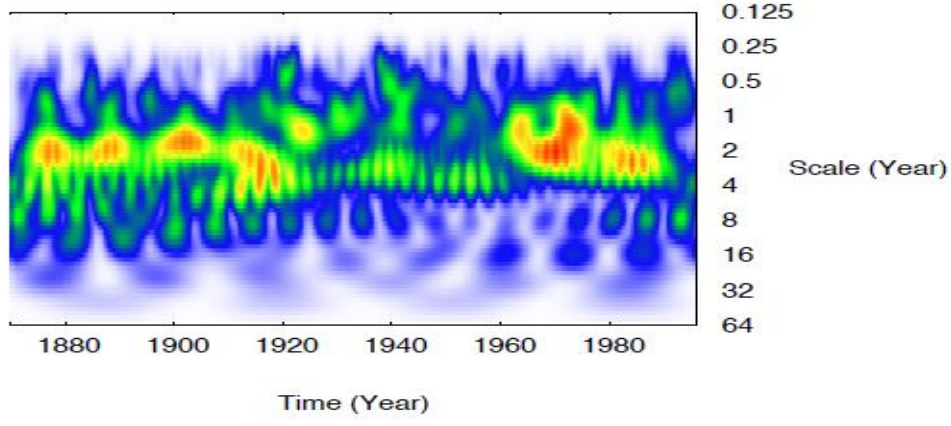

(d) PDE transform using 8th order PDE.

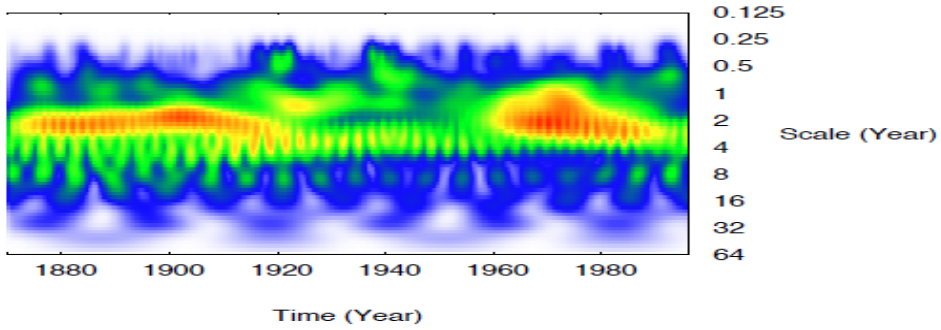

(e) PDE transform using 20th order PDE.

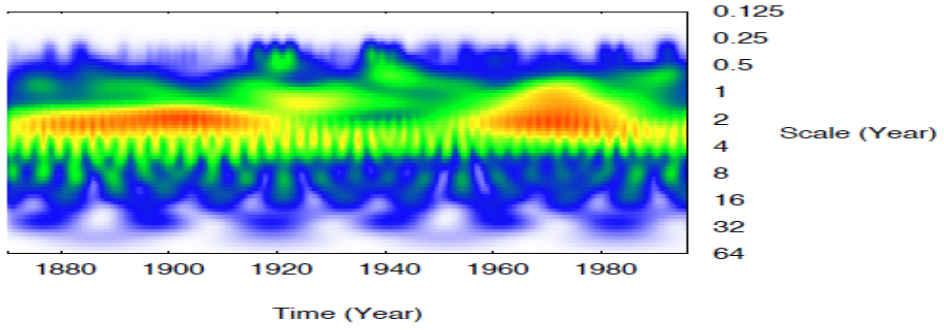

(f) PDE transform using 40th order PDE.

PDE transform based correlations

(a) Original Barbara image.

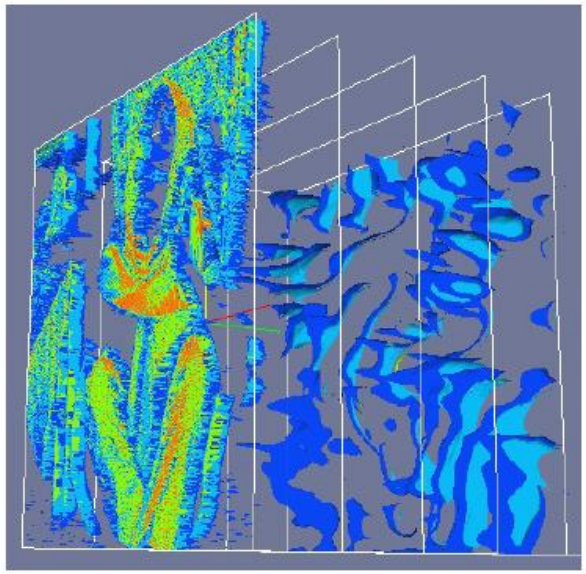

(b) 4D density of the Barbara image.

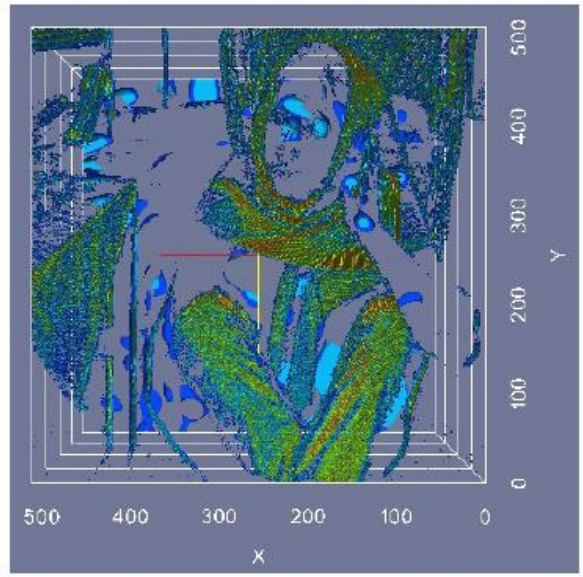

(c) Front view of the Figure 8(b).

(d) Original camera man image.

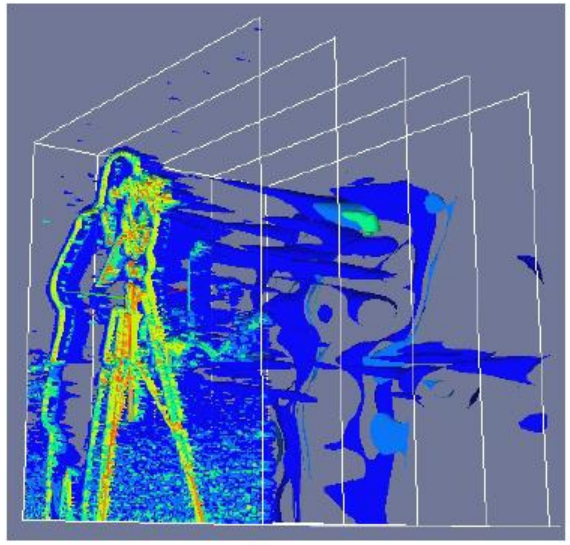

(e) 4D density of the camera man image.

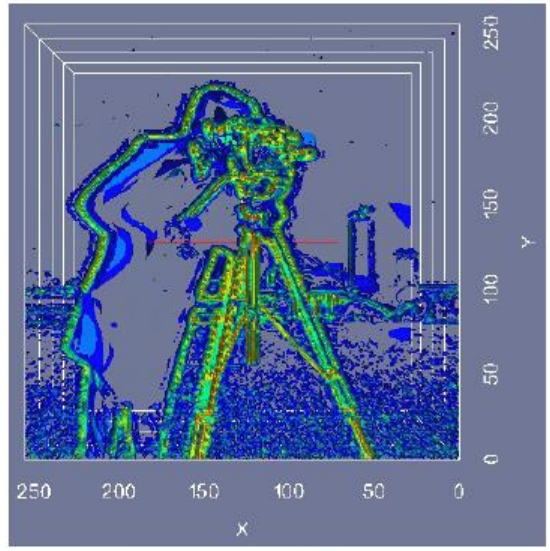

(f) Front view of the Figure 8(e).

Wavelet transform vs PDE transform

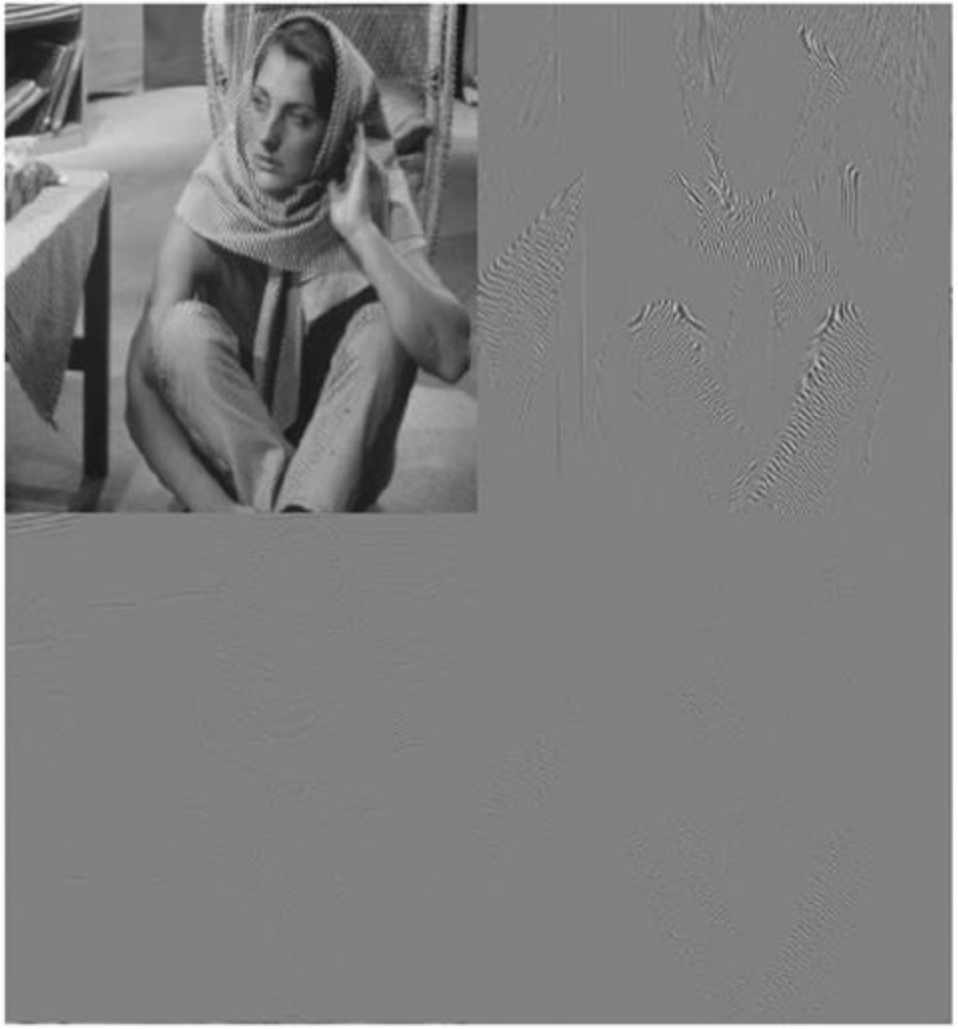

Wavelet transform

PDE transform

Adaptive PDE transform based local statistical analysis

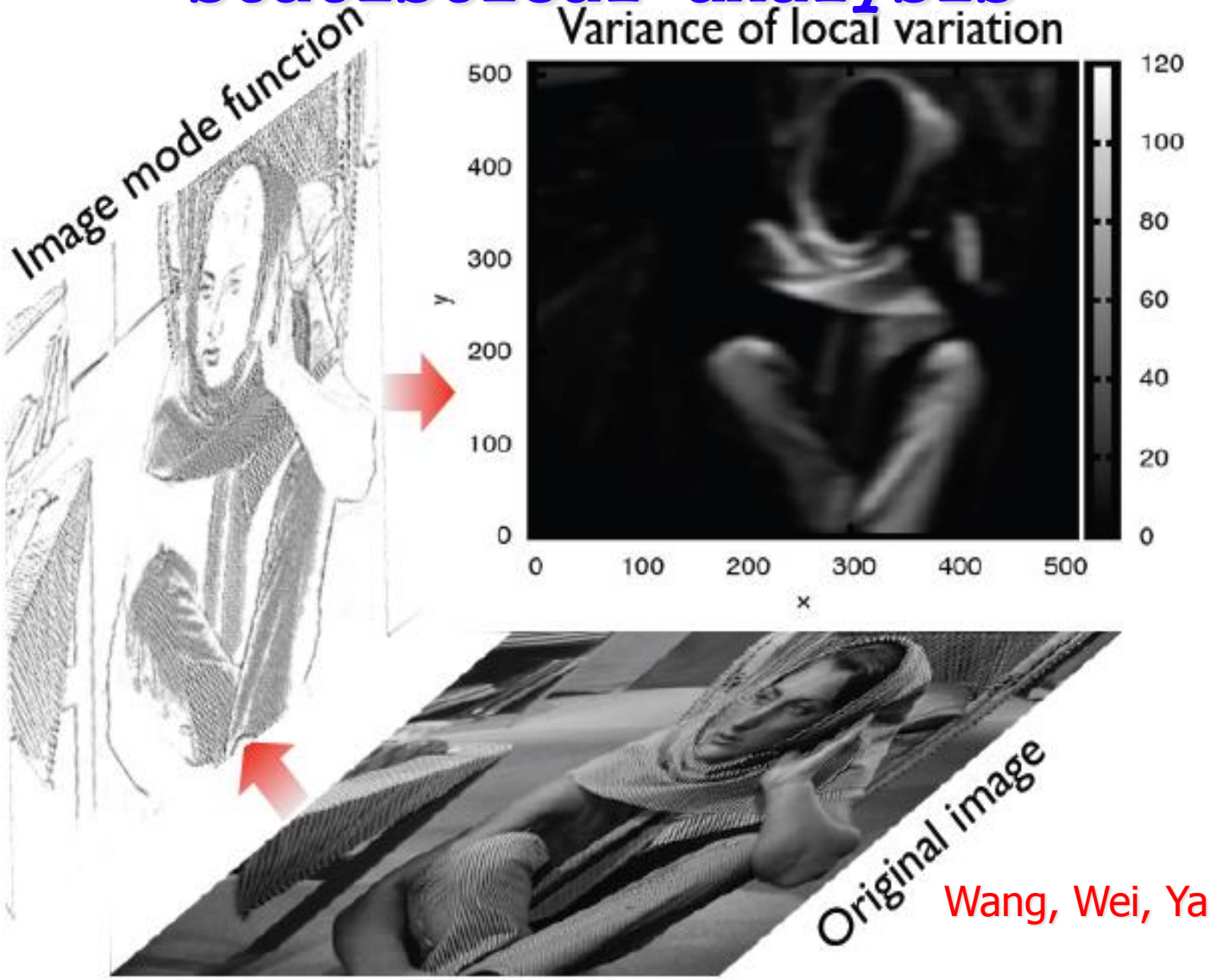

Wang, Wei, Yang, IJBI, 2012

Figure 4: Adaptive PDE transform for selective texture extraction in the Barbara image. The variance of the local variation is shown in the top chart.

(a) Original image.

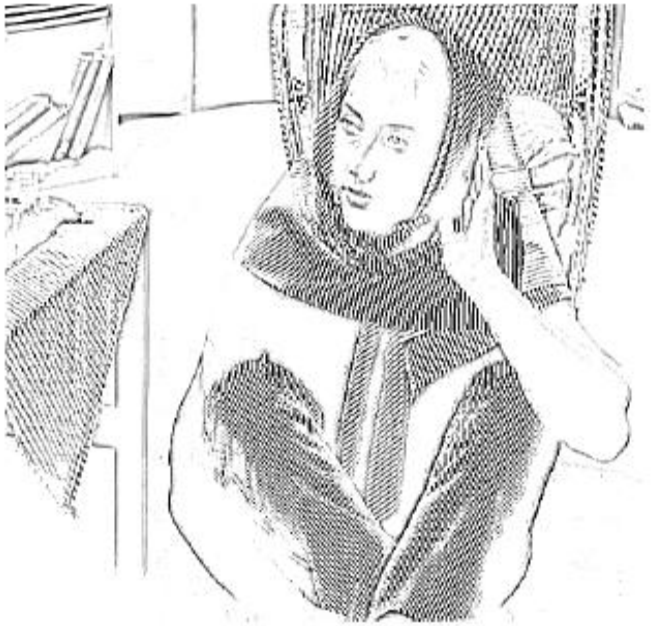

(b) Image mode function.

(c) Texture 1

(d) Texture 2

Adaptive PDE transform for texture analysis

Wang, Wei, Yang, IJBI, 2012

(a) Original image.

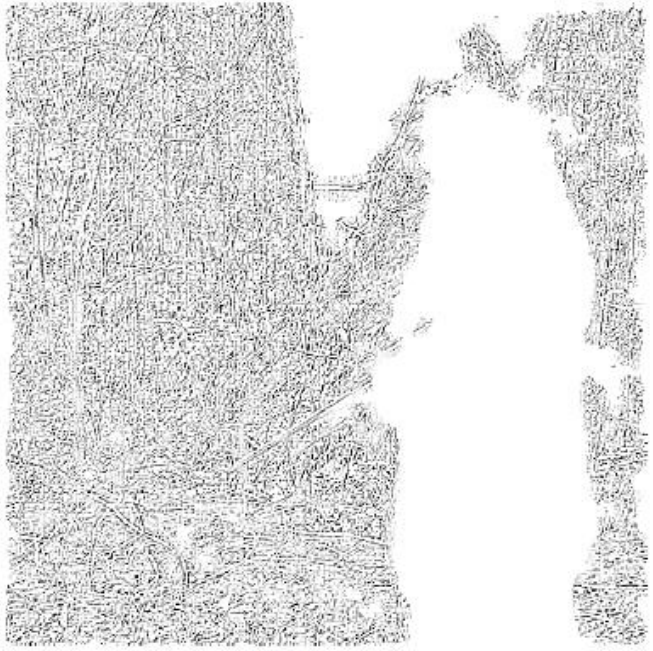

(b) Texture 1

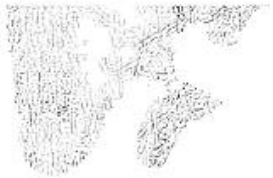

(c) Texture 2

(d) Texture 3

Adaptive PDE transform for sniper identification

Wang, Wei, Yang,
IJBI, 2012

PDE transform for texture analysis

(a) Original image.

(b) Mode function.

(c) Extracted texture.

Figure 3: Extraction and separation of texts, background watermark, and textures of image 3(a). Shown in the3(b) and 3(c) are the image mode function and extracted texture using the proposed adaptive PDE transform.

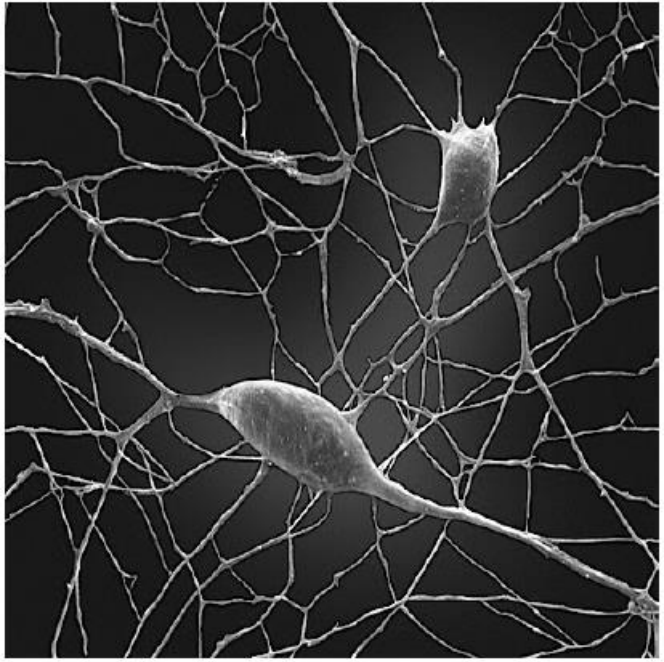

(a) Original neuron image.

(b) Class 1 of the selective neuron skeleton.

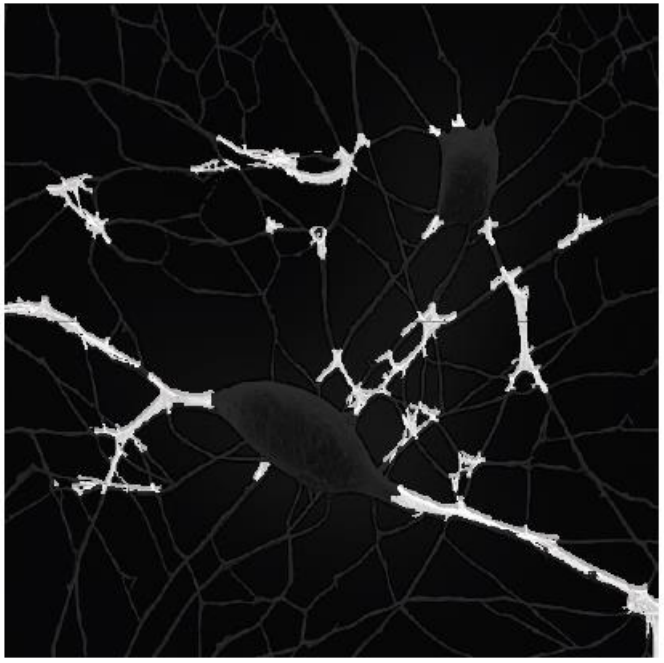

(c) Class 2 of the selective neuron skeleton.

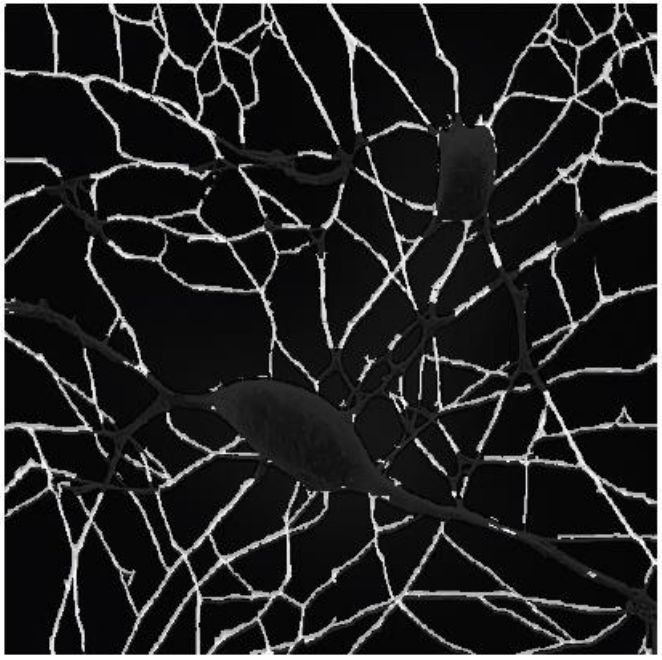

(d) Class 3 of the selective neuron skeleton.

Adaptive PDE transform for neuron classification

Wang, Wei, Yang,
IJBI, 2012

PDET for hyperbolic conservation laws

(Hu, Yang, Wei, CiCP, 2014)

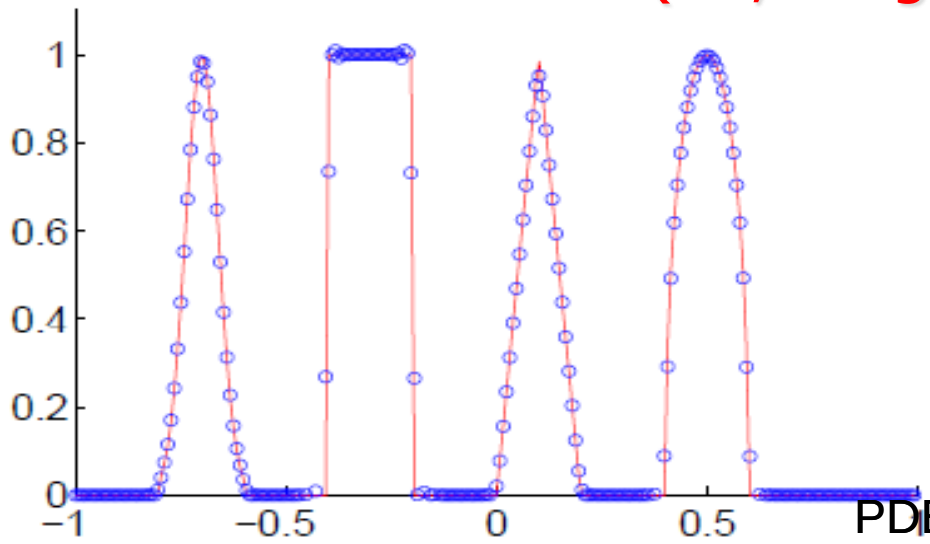

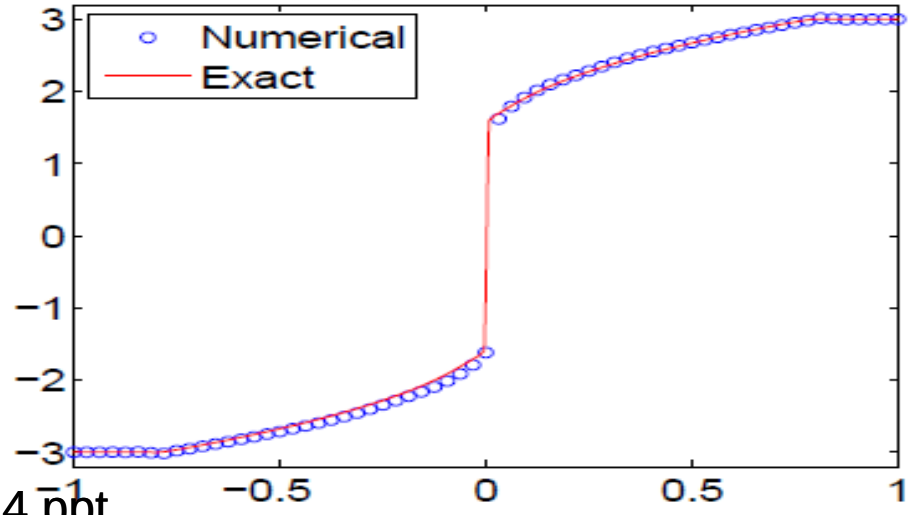

PDET2014.ppt

(c) The 6th order PDE transform (65 grid points)

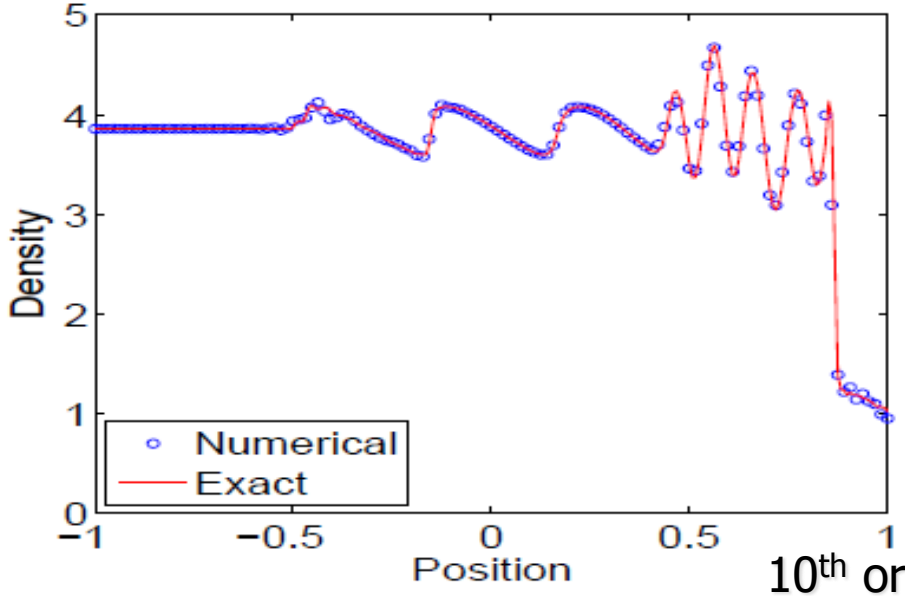

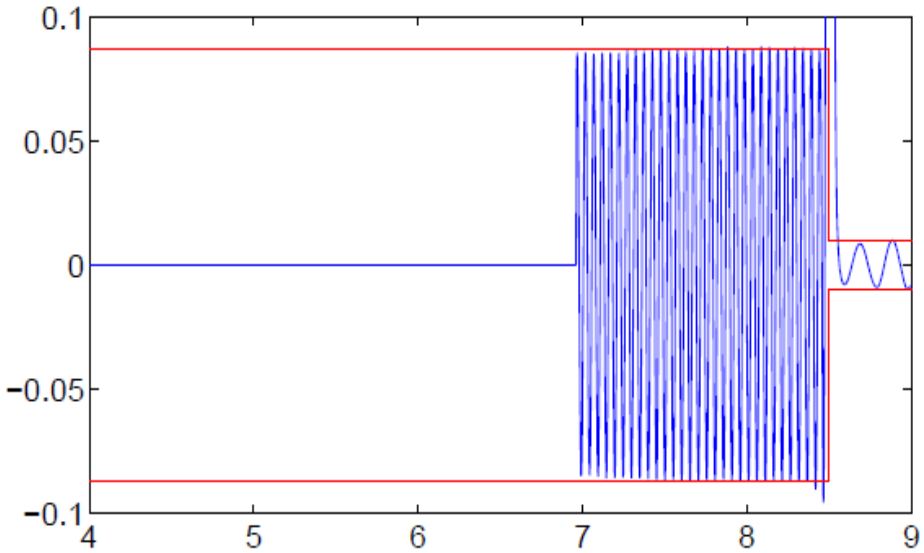

10th order PDE Transform

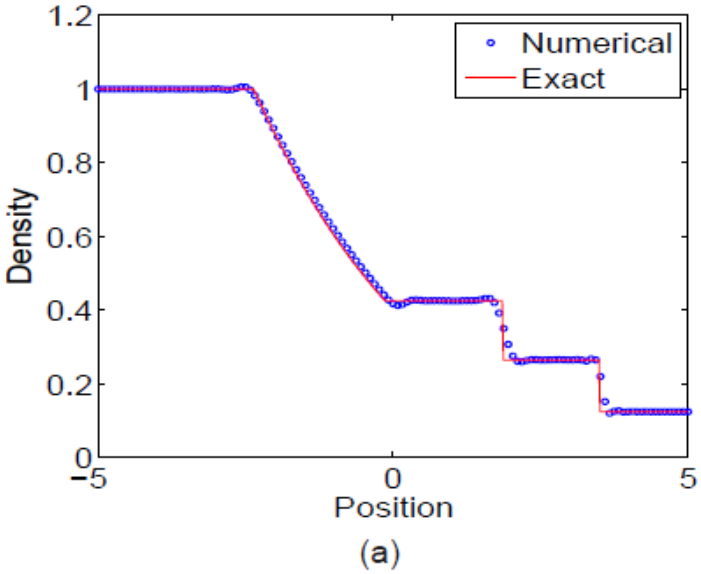

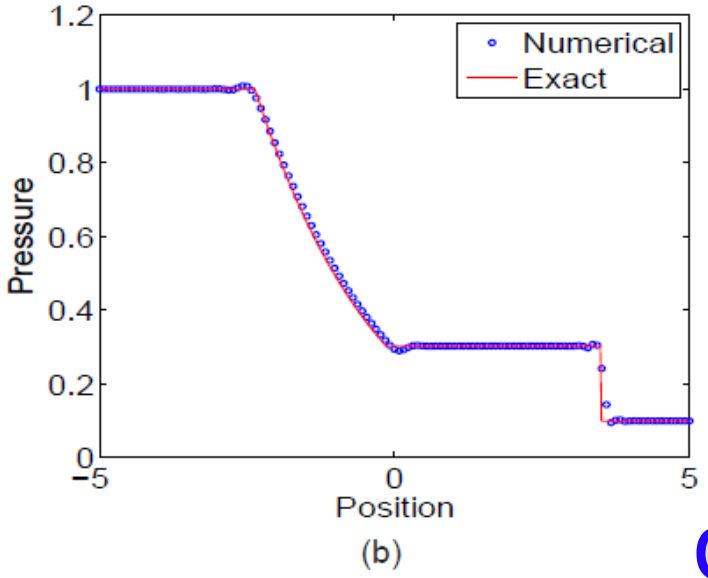

Figure 6: Numerical results from the 6th-order PDE transform for Sod's problem ($t = 1.5$, $\Delta t = 0.02$, 129 grid points). (a) Density; (b) Pressure.

PDE transform for hyperbolic conservation laws

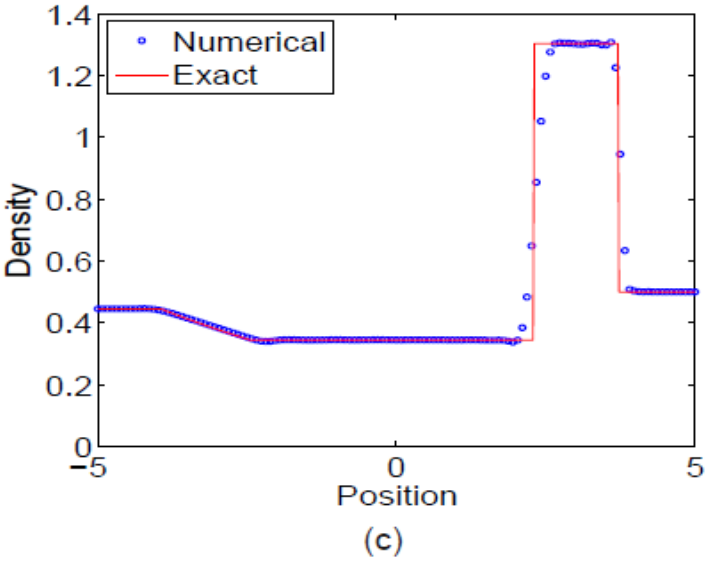

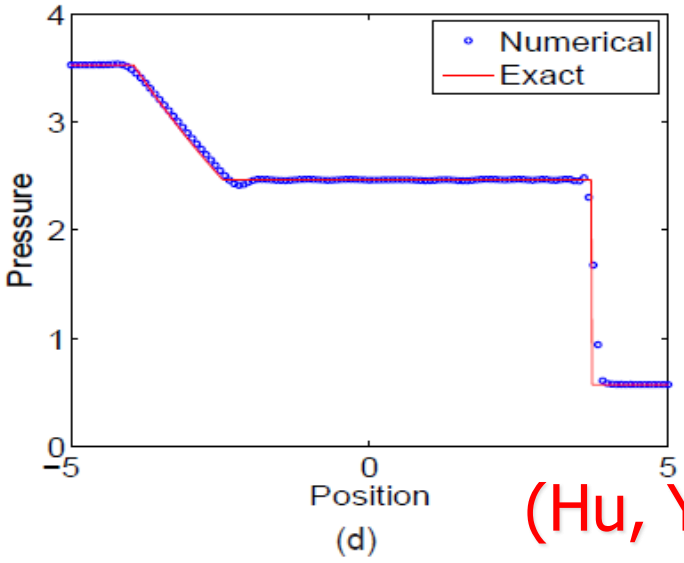

(Hu, Yang, Wei, 2012)

Figure 7: Comparison of numerical results from the 6th-order PDE transform and the FPM-RSK for Lax's problem ($t = 1.5$, $\Delta t = 0.02$, 129 grid points). (a) Density from the PDE transform; (b) Pressure from the PDE transform; (c) Density from the FPM-RSK; (d) Pressure from the FPM-RSK.

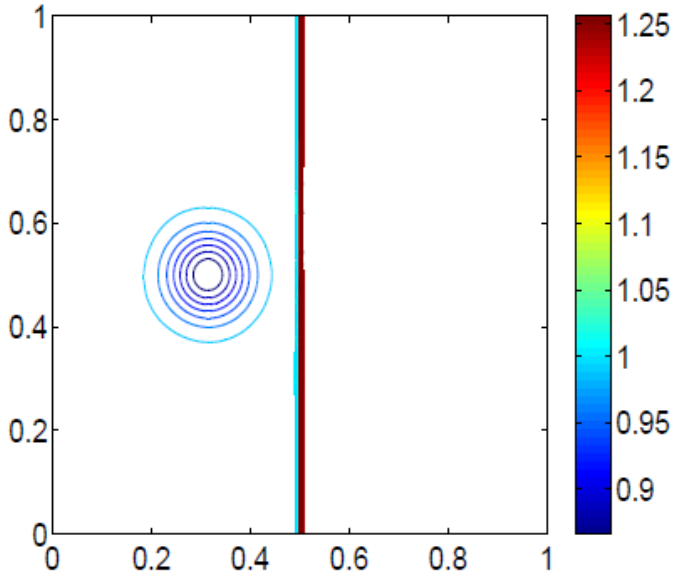

(a) $t = 0.05$

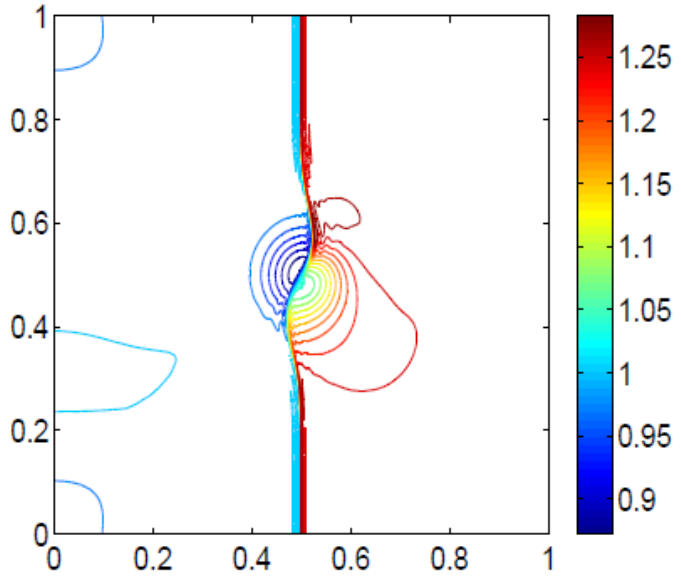

(b) $t = 0.2$

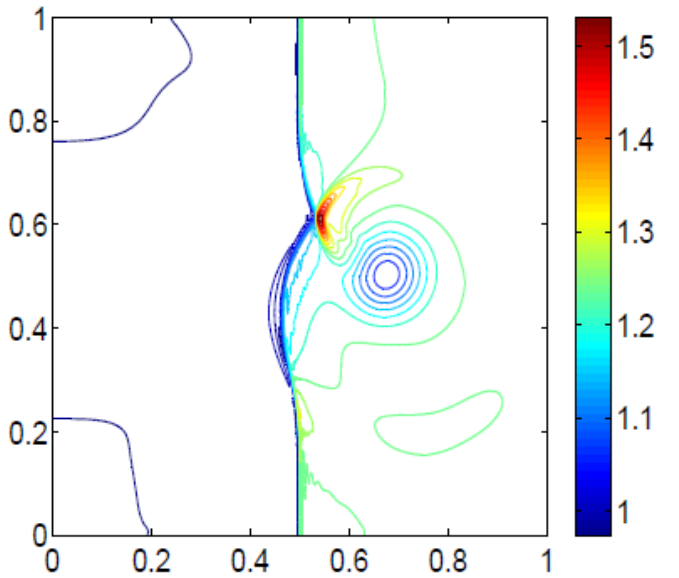

(c) $t = 0.35$

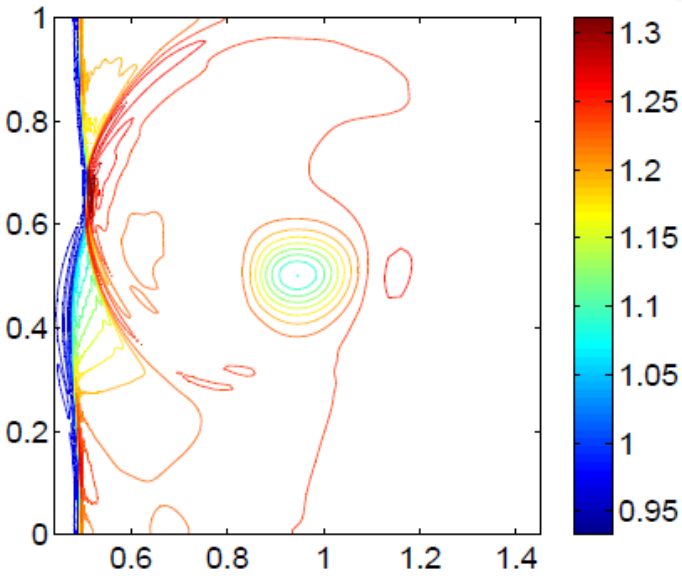

(d) $t = 0.6$

PDE transform for hyperbolic conservation laws

(Hu, Yang, Wei, 2012)

Figure 12: The pressure profile of 2D shock-vortex interaction problem from the 10th-order PDE transform (20 contours).

Comparison of Hilbert-Huang Transform, Wavelet Transform, Fourier Transform and PDE transform

Hilbert-Huang transform	Wavelet transform	Fourier transform
• Only yield the relevant functional modes • Each mode contains desired frequency range • Mode is extracted using accurate high order PDEs based band-pass filters	• Each sub-band width is totally controllable • Each mode function is determined by PDE order and evolution time • Adjustable dual temporal-frequency localization	• Each mode contains selected frequency range • Physical domain representation • Applicable for non-stationary signal, and no Gibbs oscillations
Partial Differential Equation Transform		
• Each mode is obtained by spline based lowpass filter • Instantaneous frequency is obtained for characterizing non-stationary data	• Dual time-scale analysi • Robust choice of the mother wavelet • Dilation and translation are used to capture the local characteristics	• Perfect localization in frequency space • Gibbs oscillations • Impressive improvements and applications are still occurring

Concluding remarks

- **We introduced arbitrarily high order geometric PDE for image, surface, data analysis and biomolecular modeling.**

- **We introduced coupled PDEs as high-pass filters.**

- **We introduced PDE transform as a new approach for signal, image and surface analysis.**


N Baker
(PNNL)
P Bates
(MSU)
M Feig
(MSU)
Y Tong
(MSU)
G Wang
(VPI)
J Wang
(NSF)
Y Wang
(MSU)
X Ye
(UKLR)
Shan Zhao
Alabama
Y Zhou
Colorado S
W Geng
SMU
S Yang
Houston
Duan Chen
UCC
Zhan Chen
Minnesota
S.N. Yu
Boston
Y.H. Sun
Denver